ARPA-E Report, End of Q2
Milestones 2.1 and 2.2

Abstract

Reaching the end of the second project quarter of the first year, the Oceanwater CO_2 Capture project has achieved milestones M2.1 and M2.2, which were targeted for completion at the end of this quarter. We have developed a detailed technoeconomic analysis (TEA) and quantified the tradeoff between different drivers of system cost, including electrodialyzer voltage and current density, membrane contactor pH and vacuum level, and power generation source. We have also developed a rigorous thermodynamic model of the membrane contactor to predict the carbon extraction efficiency that can be achieved at a given pH, liquid flow rate, and vacuum pressure such that operating conditions that yield high efficiencies can be identified and pursued experimentally.

We have explored TEA at different scales of CO_2 capture: one where we capture 10 kilotons of CO_2 per year (CO_2 price \$537/ton) and one where we capture 1 megaton of CO_2 per year (CO_2 price \$117/ton), putting us on track to achieve the FOA target of \$100/ton at the 1-gigaton/yr scale. At the 10-kiloton/yr scale, the capital cost (CapEx) and operating cost (OpEx) are both significant. At the 1-megaton/yr scale, OpEx dominates, consisting mostly of the electrodialysis electricity cost. We are able to achieve much lower CO_2 costs than previous estimates for oceanwater CO_2 capture mostly due to 1) improved electrodialyzer performance 2) larger scale and 3) the use of a floating platform to reduce intake/outfall costs.

We explore a variety of drivers of system cost. We find that CapEx is proportional only to electrodialyzer current density, and OpEx is proportional only to electrodialyzer voltage. Beyond 500 mA/cm^2, increasing the current density has little impact on the CO_2 price, but decreasing the voltage has benefits down to less than 1 V per cell. We also find that the steady-state partial pressure of CO_2 in our membrane contactor must be greater than 1 Torr, otherwise we incur prohibitively large vacuum pump costs. Finally, we find that if electricity is inexpensive, we can tolerate a lower capacity factor (e.g. from a variable renewable source of energy like solar or offshore wind), as low as 50%.

We explore the interplay between pH and extraction efficiency assuming either an equilibrium concentration of dissolved $CO_2(aq)$ at a given pH, or assuming that we increase the amount of CO_2 available for extraction by e.g. tailoring the liquid flow rate or catalyzing the conversion of bicarbonate into CO_2. Three scenarios stand out as directions to pursue: 1) pH 4 operation, where we extract equilibrium levels of CO_2 in the membrane contactor, 2) pH 8.1 operation, where we have catalyzed CO_2 extraction at pH 8.1 to achieve around 40% extraction efficiency, 3) operation at an intermediate pH such as pH 6, where we achieve 2-4x catalysis of CO_2 extraction rate in the membrane contactor and acidify the oceanwater slightly.

Finally, we have developed a zero-dimensional finite element model to simulate the membrane contactor, and we have mapped carbon extraction efficiency as a function of three important operating parameters: the pH of the ocean water that is fed into the contactor, the flow rate of water into the contactor, and the vacuum being applied to the contactor in order to draw off CO_2. In addition to calculating macroscopically relevant parameters like extraction efficiency at real operating points, we have also gained mechanistic insight into how the contactor can achieve substantial extraction efficiencies at near neutral or even native ocean pH. We have identified the rate-limiting chemical reactions that must occur for HCO_3^- to transform into CO_2, and with this mechanistic understanding we integrate catalysts that are targeted toward these rate-limiting chemistries in the future of the project.

Milestones Overview

M2.1 TEA trade-off analysis on expended operational design space: Detailed TEA that allows precise quantitative target metrics for the following most critical drivers of overall system cost: electrodialyzer current density, electrodialyzer voltage, membrane contactor operating pH, membrane contactor CO_2 removal rate, and three different power generation sources (solar, solar-battery, grid assisted renewables). This ensures that target values for milestones are precise and will be used to inform future system designs.

Status: *Complete*

M2.2 Thermodynamic system trade-off analysis: Perform thermodynamic analysis of dissolved CO2 dependence on pH. Use the data to analyze tradeoff between the required pH shift (energy requirement for electrodialysis) vs. the required CO2 partial pressure at the headspace over the saturated solution (energy requirement for vacuum pumping for CO2 stripping).

Status: *Complete*

1. Summary of Detailed Technoeconomic Analysis.

We build off our initial TEA to create a detailed TEA for our oceanwater CO_2 capture system.

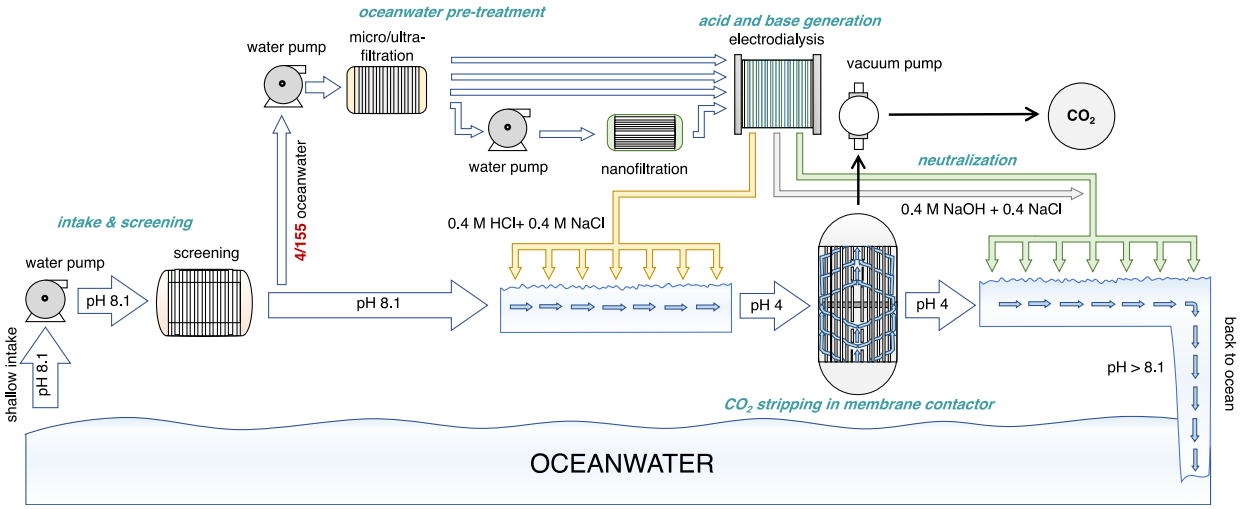

Figure 1. Schematic of the off-shore, stand-alone oceanwater CO_2 capture system.

The system design is similar to that described in our proposal (Fig. 1). We break the system down into six process steps: 1) intake, 2) screening, 3) micro/ultrafiltration, 4) nanofiltration, 5) electrodialysis, and 6) CO_2 stripping. Only a small fraction of the oceanwater (<1%) goes through steps 3–5. Key parameters and assumptions used in our TEA are described in Table 1.

Item	Cost		Parameter	Value
Centrifugal Pump (27,000 m^3/day)	$42,000		Oceanwater target pH**	4
Electrodialysis membrane cost	$0.05/$cm^2$		Membrane contactor efficiency	90%
Membrane contactor cost (1,920 m^3 oceanwater/day)	$6600		Electrodialyzer current density**	500 mA/cm^2
Vacuum pump cost (240,000 m^3/day)	$252,000		Electrodialyzer voltage**	2.5 V per cell
Intake piping* (400,000 m^3/day)	$420,000		Liquid ring vacuum pump base pressure**	35 Torr
Microscreening* (400,000 m^3/day)	$3,247,000		Scale	10 kiloton/yr (current) 1 megaton/yr (future)
Microfiltration* (10,000 m^3/day)	$1,555,000		Electricity price	$0.04/kWh (current) $0.04/kWh (future)
Nanofiltration (3,000 m^3/day)	$135,000		Labor cost (12.5 full-time employees at 10-kiloton/yr scale)	$40,000/year average salary

Table 1. Key costs and parameter values. All cash flow-related parameters are the same as (*1*).
* estimated from desalination costs (*2*)
** to be varied in future sections of this report

For our initial TEA, we examine pH 4 operation, with an electrodialyzer operating at 500 mA/cm^2 and 2.5 V per cell, and a membrane contactor operating at 90% CO_2 capture efficiency. Different pH and electrodialyzer performance values are discussed in sections 2–8.

We explore two different scenarios in our TEA. In our "current" scenario, we assume we capture 10 kilotons of CO_2 per year (requiring an oceanwater flow rate similar to currently operating desalination plants), and we assume an electricity price of $0.04/kWh. In our "future" scenario, we assume we can capture 1 megaton of CO_2 per year, and we assume an electricity price of $0.02/kWh. Since we take many of our inputs from the desalination industry, we assume capital costs are accurate at the 10-kiloton/yr scale. To scale capital cost up to the 1-megaton/yr scale, we use the commonly-adopted 6/10 rule:

$$C_2 = C_1 \left(\frac{S_2}{S_1}\right)^{6/10}$$

where C_1, C_2 are the costs at the initial and final scale and S_1, S_2 are the sizes of the initial and final scales. We assume electricity usage and costs are the same across all scales, and we scale up labor costs with a ¼ scaling exponent (*3*).

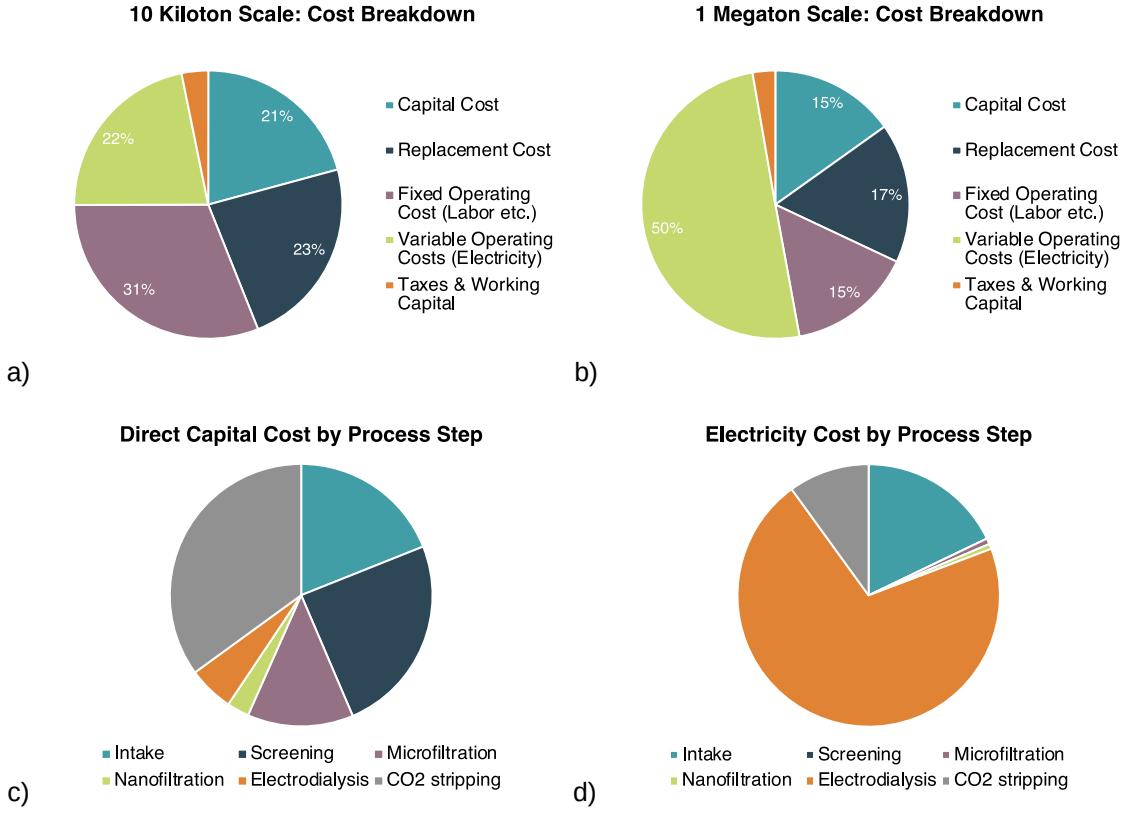

Figure 2. a) and b) Cost breakdown between CapEx, OpEx, and other components at the 10-kiloton/yr(a) and 1-megaton/yr (b) scale. c) CapEx breakdown by process step. d) Electricity cost breakdown by process step.

In our "future" scenario, the CO_2 price is $117/ton. In our "current" scenario, the CO_2 price is $537/ton. We find that CapEx and fixed OpEx (mostly labor) dominate the CO_2 cost at the 10-kiloton/yr scale. CapEx and replacements make up 44% of the CO_2 price, and fixed OpEx makes up 31% (Fig. 2a). At the 1-megaton/yr scale, electricity accounts for 50% of the CO_2 price

(Fig. 2b). Although the scale of the 1-megaton/yr scenario is 100x larger, the CapEx is only 15x larger by the 6/10 rule, making the CapEx a much less significant contributor to the CO_2 cost at larger scales.

Although CapEx and electricity scale differently from each other, the breakdown by process step is the same within each category. CO_2 stripping costs, including membrane contactors and vacuum pumps, dominate the capital cost at both the 1-megaton/yr and the 10-kiloton/yr scale, followed by screening and intake (Fig. 2c). Microfiltration, nanofiltration, and electrodialysis represent relatively small contributions to the capital cost. This demonstrates that our scheme to pass only a small fraction of the oceanwater through the filtration and acidification process successfully reduces cost.

The electrodialysis electricity dominates the electricity cost (Fig. 2d). Intake and CO_2 stripping also contribute to electricity usage, but not nearly to the same extent.

2. Comparison to Previous Work.

To ensure our TEA is accurate, we compare our results to previous work. In 2018, Eisaman *et al* examined a similar oceanwater CO_2 capture system that relied on electrodialysis to acidify the oceanwater (*4*). They reported a best-case cost of $436/ton for co-location with a desalination plant, and a best-case cost of $1389/ton for a standalone plant. Our estimated cost of $117/ton is significantly smaller than theirs.

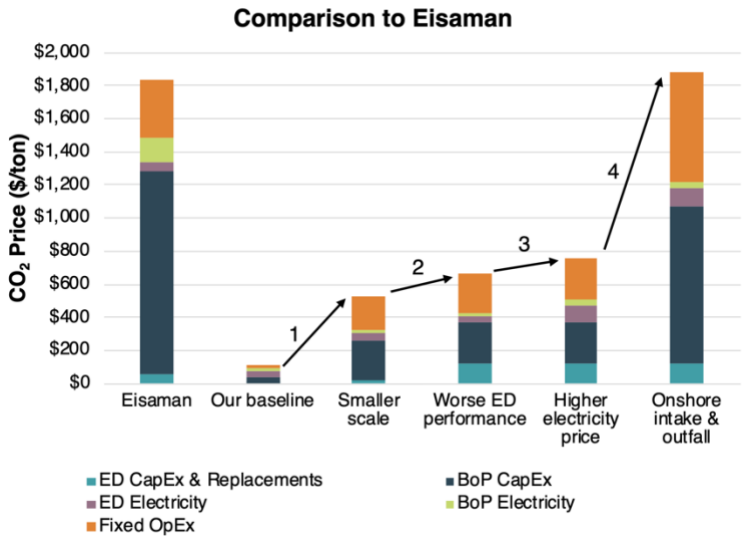

Figure 3. Comparing the CO_2 resulting from TEA of our system to a previously reported CO_2 cost from oceanwater CO_2 capture.

We achieve much lower CO_2 prices than previous papers mostly due to 1) improved electrodialyzer performance 2) larger scale and 3) the use of a floating platform to reduce intake/outfall costs (Fig 3). The arrows in the figure correspond to modifications to our system to match the cost reported by Eisaman *et al*: 1) decreasing the scale from 1 megaton/yr to 7.7 kiloton/yr, 2) decreasing the electrodialyzer current density from 500 mA/cm^2 to 100 mA/cm^2, 3) increasing the electricity cost from $0.02/kWh to $0.04/kWh, and 4) assuming 20x higher intake/outfall costs due to onshore intake and outfall as opposed to a floating platform.

The match between our predicted CO_2 price with these modifications is a good "sanity check" to confirm the accuracy of our TEA.

3. Electrodialyzer Current Density and Voltage.

To ensure that target values for milestones are precise, we sweep the electrodialyzer current density and voltage in our TEA and calculate the resulting CO_2 price.

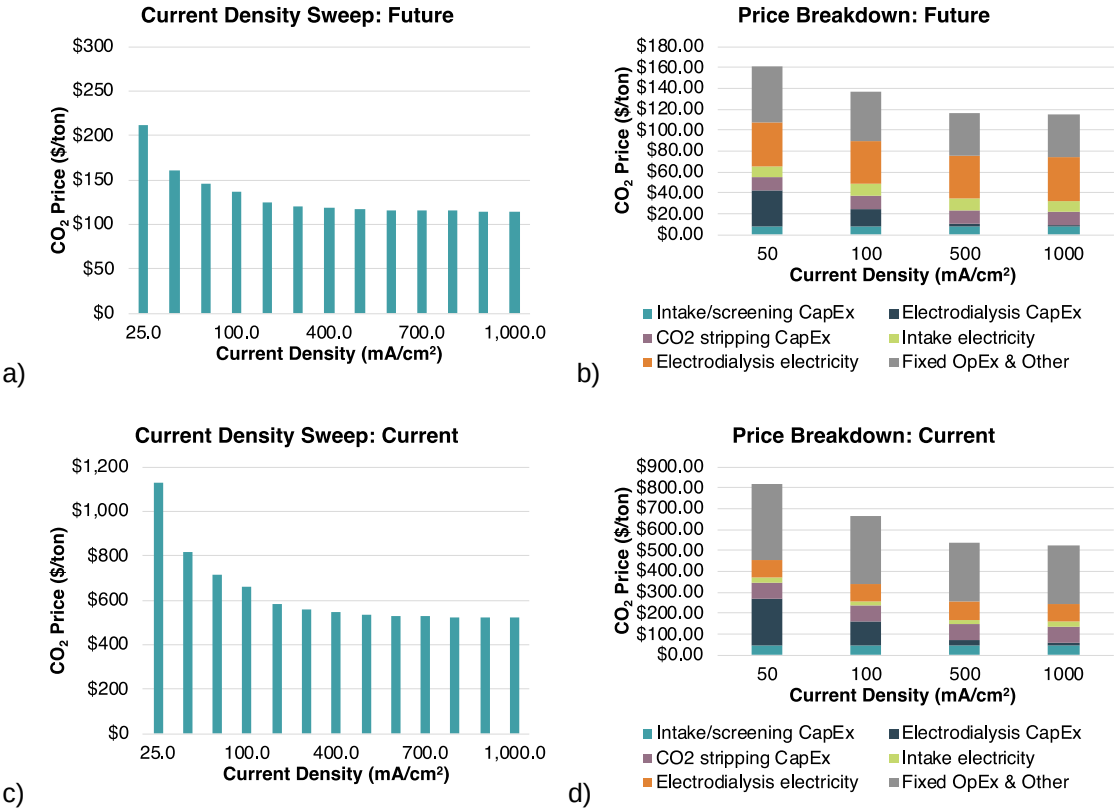

Figure 4. CO_2 price sweeping over electrodialyzer current density. a) and b) "Future" scenario (1-megaton/yr scale, \$0.02/kWh electricity price), current density sweep and breakdown by process step and CapEx/OpEx. c) and d) "Current" scenario (10-kiloton/yr scale, \$0.04/kWh electricity price).

Current Density

The electrodialyzer CapEx only depends on the electrodialyzer current density and not on voltage. The electrodialysis capital cost is given by (*1*):

$$\$ = \frac{\$}{cm^2} \cdot \frac{1}{j} \cdot F \cdot x \cdot [H^+]_{add,pH=0.4} \cdot \frac{Low}{s}$$

where $\frac{\$}{cm^2}$ is the membrane cost per unit area, j is the current density, F is the Faraday constant, x is the fraction of oceanwater that is acidified to pH 0.4, $[H^+]_{add,pH=0.4}$ is the H^+ produced by electrodialysis, and $\frac{Low}{s}$ is the oceanwater flow rate. When we sweep the current density, the main effect is therefore to the electrodialyzer CapEx. This makes sense intuitively, as a higher current density creates more protons and the protons needed in a given time determines the necessary size of the electrodialzyer unit. In contrast, electrodialyzer electricity usage per ton

CO_2 does not depend on the current density, as a higher current density would yield more CO_2 but would not change the per-ton CO_2 electricity usage.

When we sweep the current density, we see that there are diminishing returns to increasing the current density above 500 mA/cm^2 at the 1-megaton/yr scale, as the CO_2 price plateaus around \$115/ton close to 500 mA/cm^2 (Fig. 4a). Above 500 mA/cm^2, the electrodialyzer CapEx (dark blue bars in Fig. 4b) becomes negligible. The same finding holds at the 10-kiloton/yr scale, though the benefit of increasing current density is greater at current densities less than 500 mA/cm^2 (Fig. 4c-d).

The finding that there is no benefit to CO_2 cost upon increasing current density beyond 500 mA/cm^2 suggests that we should revise our target current density down from 1 A/cm^2 to 500 mA/cm^2.

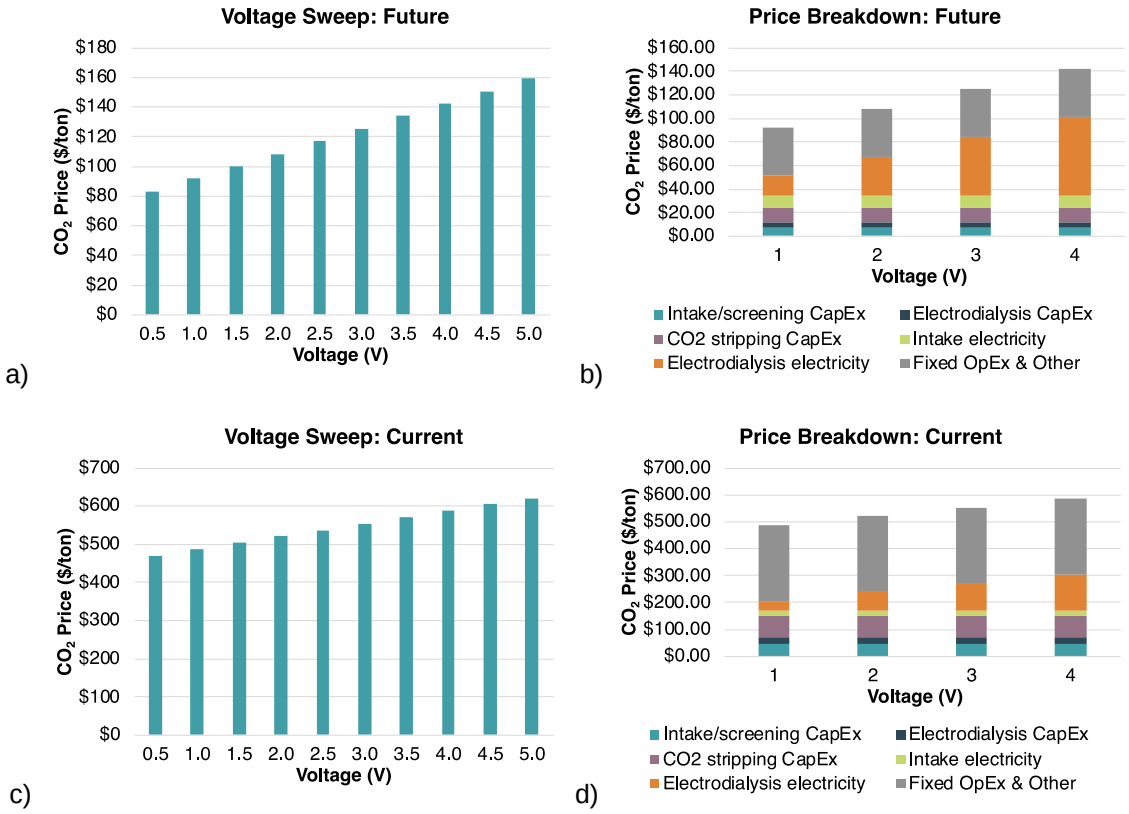

Figure 5. CO_2 price sweeping over electrodialyzer voltage. a) and b) "Future" scenario (1-megaton/yr scale, \$0.02/kWh electricity price), voltage sweep and breakdown by process step and CapEx/OpEx. c) and d) "Current" scenario (10-kiloton/yr scale, \$0.04/kWh electricity price).

Voltage

The electrodialyzer electricity cost (the main contributor to OpEx) only depends on the electrodialyzer voltage and not on the current density. The electrodialysis energy usage is given by (*1*):

$$\frac{J}{kg_{CO_2}} = V \cdot F \cdot x \cdot [H^+]_{add,pH=0.4} \cdot \frac{L_{OW}}{kg_{CO_2}}$$

where V is the electrodialyzer voltage. The electrodialysis CapEx does not depend on voltage, as the applied voltage does not increase the amount of membrane area needed.

At the 1-megaton/yr scale, reducing the voltage reduces the CO_2 price monotonically (Fig. 5a). The electrodialysis electricity OpEx alone varies with voltage, and remains significant even at 1V (Fig 5b). This finding also holds at the 10-kiloton/yr scale, though the effect is less significant, since the CapEx dominates the 10-kiloton/yr scale whereas the electricity cost dominates the 1-megaton/yr scale (Fig. 5c-d), an effect that is even more drastic at the 1-gigaton/yr scale.

The finding that any reductions to voltage decrease the CO_2 price suggest that we should retain our ambitious targets for electrodialyzer voltage.

4. Power Generation Sources.

We explore different potential power generation sources by continuously varying the electricity price and the capacity factor and calculating the CO_2 price at each point. In this section and the following, we are exploring the "future" scenario (1-megaton/yr scale).

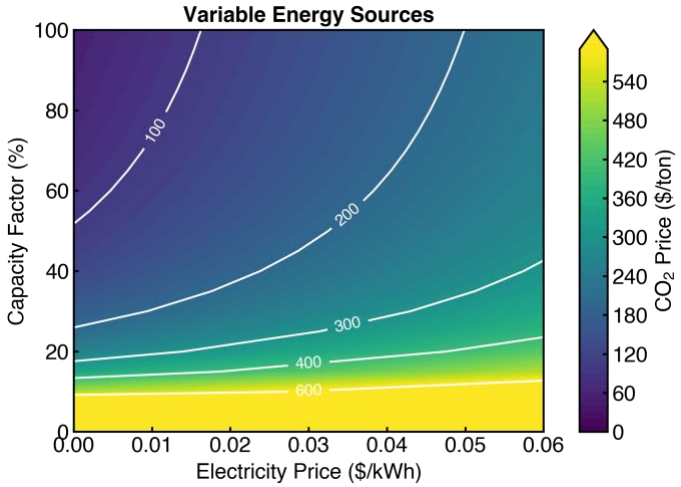

Figure 6. CO_2 price with different power generation sources, characterized by different electricity prices and capacity factors (modeled assuming "future" scenario).

We presume that at some point in the future, increased penetration of renewables on the grid may eventually lead to a need for curtailment: using or wasting extra electricity when wind and solar are overproducing to balance the grid. In this scenario, there may be a time in which consumers can access free electricity at certain times of the day, or even when consumers are paid to use electricity.

If electricity is free, we find that we can have capacity factors as low as 50% – meaning our CO_2 capture system would only be operating on average half the time over the course of a year – and still achieve less than \$100/ton CO_2 price (Fig. 6). If we are paid to use electricity to optimize the grid load, we can have even lower capacity factors. At a price of \$0.02/kWh, capacity factors of 60-80% are likely tolerable while retaining a CO_2 price close to \$100/ton. This suggests that a combined floating photovoltaic array plus offshore wind system could be a viable choice for powering our offshore oceanwater CO_2 capture system.

5. Vacuum Level in Membrane Contactor and CO_2 Removal Rate.

To inform future system design, we vary the base pressure of the vacuum pump pulling the CO_2 off the membrane contactor and calculate the CO_2 cost.

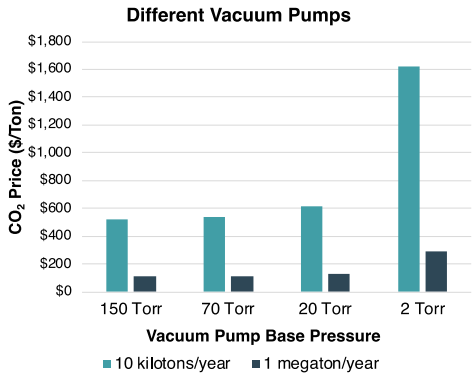

Figure 7. Effect of vacuum pump base pressure on CO_2 price (modeled assuming "future" scenario).

We find that the CO_2 cost is very sensitive to the level of vacuum in the membrane contactor (Fig. 7). This is because at lower base pressures, we have lower CO_2 partial pressures, and we need to pump a larger volume of gas out of the contactor to achieve the same molar flow rate of CO_2 out of the chamber. Most pumps have a maximum volumetric flow rate, since they are positive displacement pumps (they remove a set volume of gas over and over). At lower partial pressures and the same *volumetric* flow rate, the *molar* flow rate of CO_2 becomes much smaller due to the ideal gas law. Therefore, we would need about 10x as many pumps with the same maximum volumetric flow rate to get the same CO_2 throughput if we reduced the base pressure from 10 Torr to 1 Torr. This effect becomes significant around 1 Torr, suggesting that we should only look at operating vacuum pumps at base pressures of 1 Torr or higher.

6. Membrane Contactor Operating pH in Equilibrium.

Finally, we examine the effect of changing the operating pH of our membrane contactor. Carbon exists in seawater at a concentration of ~2 mM as dissolved inorganic carbon (DIC). Depending on pH, the DIC can take a number of different forms: carbonate (at high pH), bicarbonate (at intermediate pH), or dissolved CO_2 (at low pH). If we acidify our oceanwater from its native value of close to 8.1, we can shift the DIC balance away from bicarbonate and towards dissolved CO_2.

We can determine how many moles of H^+ we need to produce in the electrodialyzer and add to our main oceanwater stream to extract 1 mole of CO_2. At each pH, we can calculate the equilibrium concentrations of each of the DIC-related species (Fig. 8a). We can then keep track of charge balance to figure out how many moles of H^+ need to be added to get from the oceanwater pH, pH 8.1, to a new pH, such as pH 4:

$$[H^+]_{added} = \Delta[H^+] - (\Delta[HCO_3^-] + 2\Delta[CO_3^{2-}] + \Delta[OH^-])$$

where the delta represents the concentration at pH 4 minus the concentration at pH 8.1, so a positive $[H^+]_{added}$ means that protons have been added to get from pH 8.1 to pH 4. Note that $[H^+]_{added}$ does not equal the concentration of protons at pH 4, since some of the protons added go to converting bicarbonate to CO_2 rather than remaining in the solution.

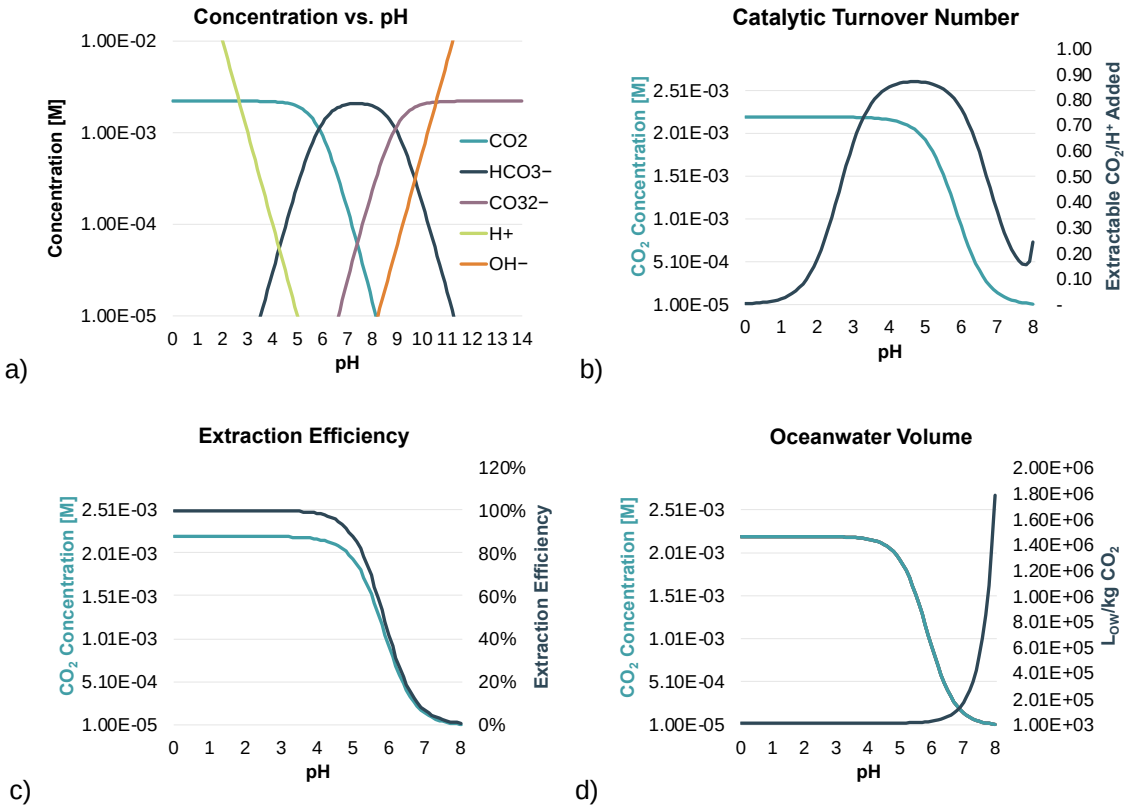

Figure 8. a) Balance between different DIC species at different pH in oceanwater. b) Catalytic turnover number, or extractable dissolved CO_2(aq) per H^+ added, as a function of pH. c) Dissolved CO_2(aq) extraction efficiency, assuming that only dissolved CO_2(aq) can be extracted. d) Oceanwater volume needed to extract a given amount of dissolved CO_2(aq).

Our collaboration has defined a key metric for our oceanwater CO_2 capture system, the *Catalytic Turnover Number*, which is the ratio between moles of CO_2 extracted and moles of H^+ added. This can be calculated from the equilibrium concentration of CO_2, the number of protons added to achieve a given membrane contactor pH, and a *Catalytic Turnover Factor* F_{CT}:

$$CTN = \frac{[CO_2]}{[H^+]_{added}} = F_{CT}\frac{[CO_2]_{pH_{MC}}}{[H^+]_{added}}$$

If only equilibrium dissolved CO_2(aq) can be extracted, $F_{CT} = 1$. Under steady-state operation with liquids constantly flowing through the reactor and/or if the reaction to CO_2 is catalyzed, F_{CT} can be greater than or less than 1.

Assuming that only equilibrium dissolved CO_2(aq) can be extracted, i.e. $F_{CT} = 1$, the CTN peaks between pH 4 and pH 5.5, since the dissolved CO_2(aq) concentration is increasing with every proton added (Fig. 8b). Below pH 4, the dissolved CO_2(aq) concentration saturates and protons added go towards acidifying the solution, i.e. protonating water, so the CTN drops. Above pH 5.5, some of the protons go towards converting carbonate into bicarbonate, so the CTN also drops. This suggests that we are most effectively utilizing our electrodialyzer in the pH 4–5.5 range, as almost every proton added translates to formation of a dissolved CO_2(aq) molecule.

We will first analyze the effect of pH assuming $F_{CT} = 1$, meaning we assume that we can extract 100% of the dissolved CO_2(aq) in oceanwater with the efficiency of the membrane

contactor η_{MC}. This analysis assumes zero chemical interconversion of other DIC into CO_2(aq) as it is removed. The extraction efficiency is then defined as:

$$\eta_{\text{extract}} = \frac{[CO_2]_{\text{pH}_{\text{MC}}}}{[\text{DIC}]} \cdot \eta_{MC}$$

which is equal to the percentage of the DIC that is extracted as CO_2. Below pH 4.5, the extraction efficiency approaches unity, as all of the DIC in the solution has been converted to dissolved CO_2(aq) (Fig. 8c).

We can also calculate the volume of oceanwater we need to process to extract a certain amount of dissolved CO_2(aq). This is given by:

$$\frac{\text{kg}_{CO_2}}{\text{L}_{\text{OW}}} = [\text{DIC}] \cdot \eta_{\text{extract}} \cdot \text{M}_{CO_2}$$

where M_{CO_2} is the molar mass of CO_2. Assuming $\text{F}_{\text{CT}} = 1$, the amount of oceanwater we need to process to extract a certain volume of CO_2 depends strongly on the pH. Above pH 6, the volume of oceanwater needed rises exponentially (Fig. 8d). This will also increase costs as pH increases (Fig. 9a).

7. Membrane Contactor Operating pH Out of Equilibrium.

In reality, any operating system will not only be able to extract dissolved CO_2(aq), or may not be capable of extracting all of the available dissolved CO_2(aq), because it will be operating in steady-state, possibly with some degree of catalytic reaction enhancement.

In steady-state operation, the equation above becomes rate-dependent.

$$\frac{\text{kg}_{CO_2}}{\text{L}_{\text{OW}}} \rightarrow \frac{\text{kg}_{CO_2}/\text{s}}{\text{L}_{\text{OW}}/\text{s}}$$

Instead of simply calculating the volume of oceanwater needed to extract a kilogram of CO_2 from equilibrium values, we need to know how the flow rates of oceanwater and of CO_2 affect the extraction efficiency, and thus the amount of oceanwater needed. For example, if we flow oceanwater through the reactor very quickly and pump CO_2 out very slowly, we will not be able to extract all of the dissolved CO_2(aq), even at pH 4. Our extraction efficiency will be lower than the values reported in Fig. 8c. If we let the oceanwater sit in the membrane contactor with an infinitely small flow rate and pull a vacuum, we will eventually extract all of the DIC, not just the dissolved CO_2(aq), even at a high pH. The effect of different liquid and gas flow rates on extraction efficiency will be discussed in Section 9, where we introduce a 0D reactor model that calculates the steady-state operation of our system. The operating points from this model will then be used as inputs to the TEA.

We will also observe extraction efficiency enhancement if we are able to catalyze the reactions in our membrane contactor, e.g. by speeding the conversion of bicarbonate into CO_2 with a carbonic anhydrase mimic. This can be modeled in our TEA by including a catalytic turnover factor F_{CT} that is greater than 1. This will be explored in Section 8.

8. Three Pathways to $100/ton at 1-megaton/yr Scale.

From our TEA, three scenarios stand out as directions to pursue: 1) pH 4 operation, where we extract equilibrium levels of CO_2 in the membrane contactor, 2) pH 8.1 operation, where we have catalyzed CO_2 extraction at pH 8.1 to achieve around 40% extraction efficiency, 3)

operation at an intermediate pH such as pH 6, where we achieve 2-4x catalysis of CO_2 extraction rate in membrane contactor and acidify the oceanwater slightly.

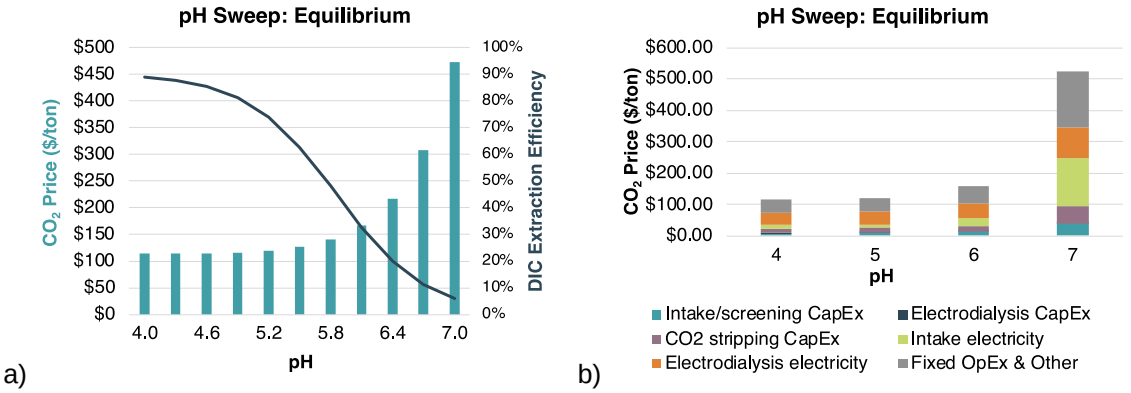

Figure 9. Scenario 1: Extracting the equilibrium concentration of dissolved CO_2(aq). Operation at pH 4 is best.

Assuming we can only extract the equilibrium concentration of dissolved CO_2(aq) at a given pH, the CO_2 price increases as pH increases due to decreased extraction efficiency (Fig. 9a). This mostly increases the intake electricity cost (green bars), since at lower extraction efficiencies, we have to process more water to extract the same amount of CO_2 (Fig. 9b). In this scenario, operating at pH 4 would be best and we would focus on improving the electrodialyzer performance by decreasing the electrodialyzer voltage at a current density of 500 mA/cm^2.

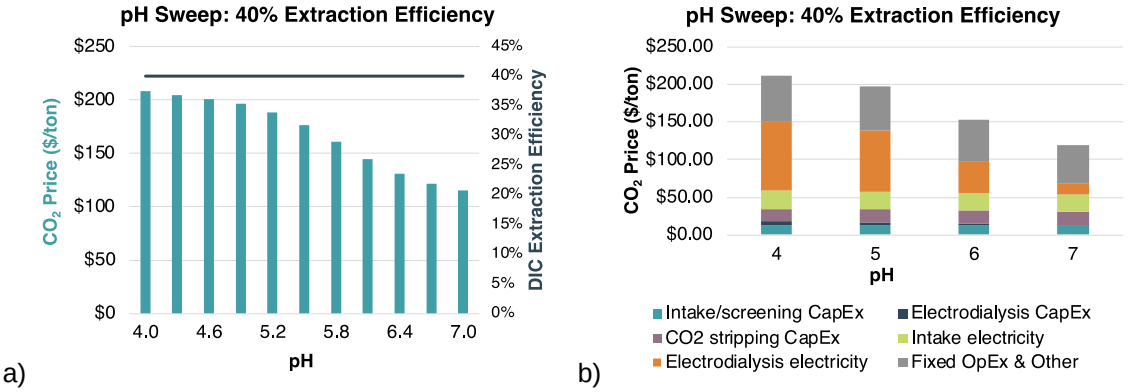

Figure 10. Scenario 2: A constant extraction efficiency of 40% is achieved by catalysis. Operation at pH 8.1 is best.

If we can achieve higher extraction efficiency at more neutral pH values via catalysis, the cost drops substantially as pH increases (Fig. 10a). As pH increases, we have to acidify a smaller fraction of the oceanwater through electrodialysis, and if we achieve the same extraction efficiency, this leads to savings in electrodialysis electricity (orange bars, Fig. 10b). In this scenario, we have catalyzed CO_2 production (e.g. with a carbonic anhydrase mimic) in the membrane contactor. If we are able to achieve extraction efficiencies close to 40% via catalysis, we may not even need an electrodialyzer, i.e. we can operate using an intake of native ocean water at pH 8.1.

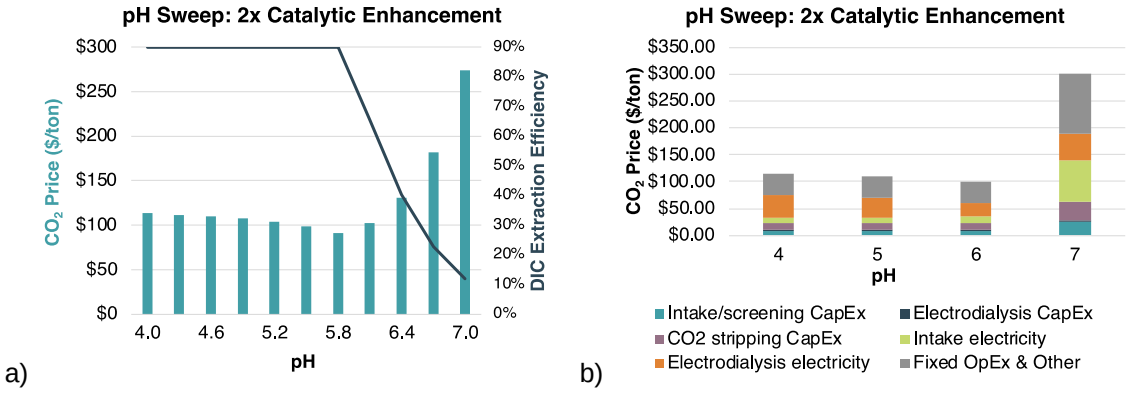

Figure 11. Scenario 3: 2x enhancement of bicarbonate to CO_2 reaction is achieved. Operation at intermediate pH is best (e.g. pH 6). The dark blue bar levels off in (a) because extraction efficiencies greater than the membrane contactor efficiency are not possible.

Intermediate pH values between 4.0 and 8.1 are worth pursuing if we can achieve some small catalytic enhancement of CO_2 production. If we can catalyze CO_2 production by a factor of 2 (e.g. with a carbonic anhydrase mimic), we can remove double the amount of CO_2 we could remove from dissolved CO_2(aq) only. This leads to lower CO_2 prices at an intermediate pH (Fig. 11a), since both the intake and electrodialysis electricity costs are low (Fig. 11b). In this scenario, we would co-optimize the membrane contactor and the electrodialyzer performance.

Together, these three scenarios suggest that there are multiple pathways to \$100/ton CO_2 capture, and that we should continue pursuing improvements in both the electrodialyzer and in the membrane contactor before deciding on a single path forwards.

9. Modeling Steady-State Operation with a 0D Model.

To model the steady-state operation of our system, we have developed a zero-dimensional finite element model to simulate the ideal performance of the membrane contactor in the absence of any limitations due to mass transfer (Fig. 12).

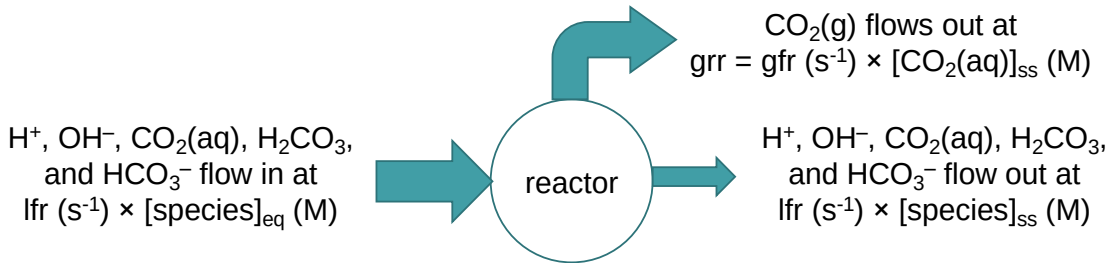

Figure 12. Our zero-dimensional finite element model indicating the species modeled and flow rates (M/s) for species in the liquid phase (lfr) and gas phase (gfr). The size of the arrows is meant to approximate relative concentrations of DIC and CO_2(g) under efficient operation. Gfr, gas flow rate. Lfr, liquid flow rate, Grr, gas reaction rate.

This model incorporates all the chemical reactions relevant to DIC speciation in oceanwater, including previously published rate constants. As inputs, the model takes the liquid flow rate of oceanwater into the contactor (assumed to be the same as the liquid flow rate out of the contactor), the gas flow rate of CO_2 out of the contactor, and the pH of the oceanwater. Once

the simulation has obtained steady-state operation, we calculate the concentration of gaseous CO_2 in the contactor and therefore its partial pressure, as well as the extraction efficiency.

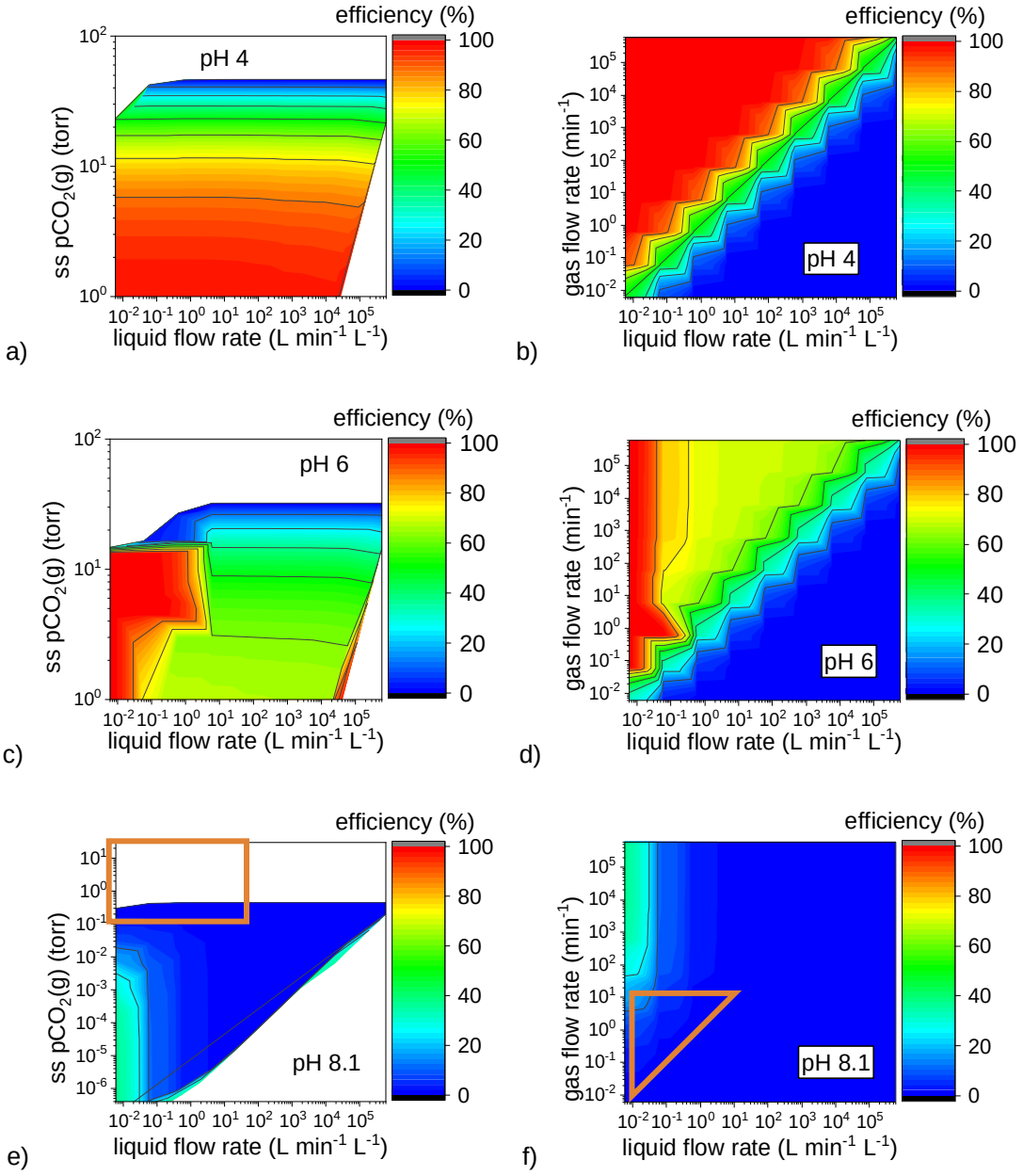

Figure 13. Extraction efficiency in the membrane contactor at three different pH values. Data in the left column are plotted as a function of the steady-state partial pressure of CO_2 in the reactor. Data in the right column are plotted as a function of the gas flow rate out of the reactor. a–b) pH 4. c–d) pH 6. e–f) pH 8.1.

We map extraction efficiency as a function of three important operating parameters: the pH of the ocean water that is fed into the contactor, the flow rate of water into the contactor, and the vacuum being applied to the contactor in order to draw off gaseous CO_2 (Fig 13). These data demonstrate that this model is imperative to understanding the real, steady-state operation of our membrane contactor, assuming zero limits due to mass transfer and no added catalysts, which we propose to design and demonstrate their efficacy later in our project.

For example, at pH 4, the equilibrium concentration of dissolved $CO_2(aq)$ is close to 100% of the DIC. However, at pressures greater than about 5 Torr, extraction efficiencies drop below 100% at all liquid flow rates (Fig. 13a–b). This could not have been predicted using the equilibrium-based analysis in Sections 7-8. In contrast, at pH 6, extraction efficiencies larger than the equilibrium concentration of dissolved $CO_2(aq)$, which is only 38%, can be observed at low liquid flow rates (Fig. 13c–d). In fact, the extraction efficiency can reach nearly 100% over a large range of CO_2 partial pressures. At pH 8.1, extraction efficiencies that exceed the equilibrium fraction of $CO_2(aq)$ are possible, but at pressures that are too low to be feasible for our project due to the vacuum pump analysis described in Section 5 (Fig. 13e–f).

Finally, we have identified the rate-limiting chemical reactions that must occur for HCO_3^- to transform into CO_2 (data not shown). This mechanistic understanding will inform our future project directions, as we aim to integrate catalysts that are targeted toward increasing the rate of these rate-limiting chemistries. The data in Fig. 13 does not include any chemical catalysis.

10. Performing TEA on Steady-State Operation Conditions.

Each point on the heat maps in Fig. 13 can be taken as an input to our TEA. The partial pressure of CO_2 in the reactor can be used to determine the necessary vacuum pump base pressure for the TEA. The extraction efficiency is already an input to the TEA, and rather than calculating it from the equilibrium fraction of DIC that is dissolved $CO_2(aq)$, we can directly input the extraction efficiency from a given point on the heat map. This extraction efficiency affects the amount of oceanwater that needs to be processed in order to extract a given amount of CO_2, as shown in Fig. 8d. For example, a reduction in extraction efficiency by half leads to a doubling of the required oceanwater throughput (and therefore the intake, screening, and membrane contactor CapEx and OpEx).

Translating the zero-dimensional liquid flow rate (lfr) and gas flow rate (gfr), both given in units of inverse time, is slightly more complex. For a given yearly CO_2 output and extraction efficiency, the gas flow rate of CO_2 out of the system and the liquid flow rate of oceanwater into the system are already defined. In the non-steady-state analysis shown in Sections 1–8, the numbers of membrane contactors and vacuum pumps are calculated assuming that each is operating at its maximum throughput. Thus, for a given CO_2 output and extraction efficiency, it is possible to calculate a minimum number of membrane contactors and vacuum pumps, as well as a corresponding ratio of lfr to gfr. The steady-state conditions specify a different lfr to gfr ratio. To incorporate this ratio, we allow the membrane contactors and vacuum pumps to operate below their maximum throughput values. For example, if the zero-dimensional model specifies a lower lfr/gfr ratio by a factor of ½, we can increase the number of membrane contactors by a factor of 2, with each operating at ½ its maximum throughput.

This analysis does not yet take into account the reactor volume (i.e. the volume of the membrane contactor), and this will be the subject of ongoing work. Scaling the relative volumes between the liquid and the gas in the reactor could yield a similar result to scaling the relative flow rates.

Based on the TEA analysis in Sections 1–8, the requirements for low CO_2 price are 1) low volume of oceanwater processed 2) vacuum pump base pressure above 1 Torr and 3) high extraction efficiency. Combined, these three criteria denote a target area in the parameter-space of our zero-dimensional simulations. We want a high vacuum pump base pressure, which is achieved by low gas flow rates. We also want our gas flow rate to be larger than the liquid flow

rate (low lfr to gfr ratio), since vacuum pumps are less expensive than membrane contactors on a per-volume basis. This criterion also generally translates to a higher extraction efficiency.

The target area for the zero-dimensional simulations is outlined in orange in Fig. 13e–f. The box (Fig. 13e) corresponds to high base pressure and low liquid flow rates, and the triangle (Fig. 13f) corresponds to low gas flow rates, and liquid flow rates that are equal or lower. These target areas are equivalent, as gas flow rate determines partial pressure.

pCO_2 (torr)	Extraction efficiency (%)	lfr (min^{-1})	gfr (min^{-1})	CO_2 Price
23	50	6	6	$182
4	91	0.6	6	$159
0.5	99	0.6	60	$483

Table 2. TEA performed on three operating points derived from the zero-dimensional model at pH 4 (Fig. 13a–b). lfr, liquid flow rate; gfr, gas flow rate. CO_2 price modeled using "future" scenario.

pCO_2 (torr)	Extraction efficiency (%)	lfr (min^{-1})	gfr (min^{-1})	CO_2 Price
30	6	6	0.6	$710
6	100	0.1	1	$118
3	63	6	6	$589

Table 3. TEA performed on three operating points derived from the zero-dimensional model at pH 6 (Fig. 13c–d). lfr, liquid flow rate; gfr, gas flow rate. CO_2 price modeled using "future" scenario.

We examine three operating points from the zero-dimensional model plots in Fig. 13 for both pH 4 and pH 6 operation (Table 2–3). At pH 4, CO_2 price is lowest at a relatively low CO_2 partial pressure of 4 Torr, since extraction efficiencies above 90% are not achievable at higher pressures. All three points selected at pH 4 have a higher CO_2 price than previously calculated in our non-steady-state TEA ($159/ton and greater, as compared to $117/ton). Surprisingly, a lower CO_2 price of $121/ton is achievable at pH 6 at a CO_2 partial pressure of 5 Torr because of the high extraction efficiency and low lfr to gfr ratio. This operating point falls in the middle of the target area described above.

Conclusions

In conclusion, we have completed a detailed TEA trade-off analysis, covering many of the drivers of system cost. From this TEA, we have refined our target values for future milestones. In particular, we plan to revise M3.1 to target an electrodialyzer current density of 500 mA/cm^2 rather than 1 A/cm^2, as we have found that improving the current density beyond 500 mA/cm^2 has no effect on CO_2 price. We continue to target low electrodialyzer voltage and pressures greater than 1 Torr in the membrane contactor, as well as catalysis to enhance the rate of CO_2 removal at high pH. Employing a zero-dimensional finite element model, we have analyzed steady-state operation of our reactor. We have integrated this steady-state model with our technoeconomic analysis and gained the capability to analyze CO_2 cost at realistic operating points of our system. We have identified several interesting future directions for system design, including 1) operating at pH 4 and achieving high extraction efficiency while using currently available membrane contactors, 2) operating at pH 8.1 and catalyzing the reaction from

bicarbonate to CO_2 to achieve 40% extraction efficiencies without any electrodialyzer, and 3) operating at an intermediate pH and enhancing extraction efficiency by either taking advantage of steady-state operating conditions at low liquid flow rates or performing moderate catalysis. We will pursue all of these directions as the project progresses.

References:

1. I. A. Digdaya *et al.*, *Nat. Commun.* **11**, 1–10 (2020).
2. N. Voutchknov, *Desalination Engineering: Planning and Design*.
3. M. Penev, G. Saur, C. Hunter, J. Zuboy, *H2A, NREL* (2018).
4. M. D. Eisaman *et al.*, *Int. J. Greenh. Gas Control*. **70**, 254–261 (2018).